

## Phase Behavior of Poly(ethylene oxide)–Poly(propylene oxide)–Poly(ethylene oxide) Triblock Copolymers in Water

Kewei Zhang and Ali Khan\*

Physical Chemistry 1, Chemical Center, Lund University, S-22100 Lund, Sweden

Received September 9, 1994; Revised Manuscript Received January 18, 1995\*

**ABSTRACT:** Phase behavior of ethylene oxide (EO)–propylene oxide (PO)–ethylene oxide triblock copolymers in water has been investigated, by using  $^2\text{H}$  NMR and polarizing microscopy, as functions of both concentration and temperature. Seven copolymers, having wide variations of composition and molecular weight, are used. It has been demonstrated that formation of liquid crystalline phases above certain polymer concentrations is a rather common feature for the EO–PO–EO triblock copolymer–water systems. The liquid crystalline phases formed are cubic, hexagonal, and lamellar phases. A cubic phase which may possess a bicontinuous-type structure has been identified. Four factors are important for controlling the phase behavior. They are molecular weight, polymer chemical composition, temperature, and concentration. A minimum molecular weight of the copolymer is needed in order to form the liquid crystalline phases. Moreover, a close relationship between the cloud point of the copolymer and the mesophase structures has been indicated.

## Introduction

EO–PO–EO (EO and PO being ethylene oxide and propylene oxide, respectively) triblock copolymers (trade name Pluronic), denoted here as  $\text{EO}_n\text{PO}_m\text{EO}_n$ , where  $n$  and  $m$  represent the number of EO and PO units, respectively, belong to the so-called amphiphilic polymers. They have attracted considerable attention in both fundamental research and practical applications. This type of polymer shows a close resemblance to the self-assembly behavior of simple nonionic surfactants of the oligo(ethylene oxide) type, with micelle formation and the formation of liquid crystalline phases. It has been established that a micelle consists of a core of PO blocks surrounded by a fringe of EO blocks, which are strongly hydrated. The critical micelle concentration (cmc) as well as the size and shape of the aggregates are found to be very sensitive to temperature. On increasing temperature, the cmc is reduced significantly and the aggregates often undergo a sphere-to-rod type transition.<sup>1,2</sup> Extensive studies have focused on micellization in dilute solutions.<sup>1–5</sup> A theoretical model based on a mean-field lattice theory has been developed for the aqueous solutions.<sup>6</sup> The micellar aggregates vs monomeric solution as well as the transition from spherical micelles to rodlike micelles are examined. On the other hand, studies on the concentrated regions are relatively unexplored.

At higher polymer concentrations, several Pluronic–water systems form liquid crystalline phases, such as lamellar, hexagonal, and cubic phases.<sup>7–9</sup> Of these, the microstructure of the cubic phase was studied for a limited number of systems.<sup>7,8</sup> A body-centered-cubic (bcc) structure was established.<sup>8</sup> The stability of other liquid crystalline phases with respect to concentration and temperature, water binding to the hydrophilic head groups, and microstructure of the liquid crystalline phases have not been studied in any detail. Structural parameters such as the molecular weight ( $M_w$ ) and polymer chemical composition, defined here by  $f = (\text{degree of polymerization for both EO blocks})/(\text{degree of polymerization for the PO midblock})$ , are important

variables influencing the micellization and microstructure of liquid crystalline phases.

In the present report, we investigate, using a water  $^2\text{H}$  NMR technique in combination with polarizing microscopy, the phase behavior of Pluronic copolymers in water as functions of both concentration and temperature. Seven copolymers, having wide variations of composition and molecular weight, are used. Of these, two systems are studied in more detail.

## Experimental Section

**Materials.** Pluronic copolymers were obtained from BASF and were used as received.  $^2\text{H}_2\text{O}$  (99.8 atom %  $^2\text{H}$ ) was purchased from AG Basel, Basel, Switzerland.

**Sample Preparation.** Samples were prepared by weighing appropriate amounts of polymer and water into 8 mm i.d. glass tubes which were flame-sealed immediately. Liquid crystalline samples were mixed by repeated centrifugation for several days, and samples in the solution regions were mixed by shaking overnight. Thoroughly mixed samples were kept at 25 °C for several days before the measurements were performed. It was found that liquid crystals formed by the polymers were softer compared to those formed by the nonionic or ionic surfactants at identical sample concentrations.

**Water  $^2\text{H}$  NMR.**  $^2\text{H}$  NMR of deuterated water is a well-established technique and has been widely used in two-component and multicomponent surfactant systems for studying the phase equilibria, for characterizing phases, and for obtaining the water binding to the head groups of surfactant molecules in liquid crystalline phases.<sup>10,11</sup> However, this method has not been applied to a great extent to study the phase behavior of the amphiphilic polymer–water systems. The deuteron nucleus has a spin quantum number of unity, and thus it possesses an electric quadrupole moment. Its NMR spectrum is dominated by the interaction of the quadrupole moment with the electric field gradients at the nucleus. In an isotropic phase, such as a micellar solution or a cubic liquid crystalline phase, this interaction is averaged to zero as a result of rapid and isotropic molecular motion, giving rise to a sharp singlet in the spectrum (Figure 1a). On the other hand, this interaction does not average to zero in an anisotropic liquid crystalline phase, such as a homogeneous lamellar or a hexagonal liquid crystal, and the spectrum splits into two equally intense peaks (Figure 1b).

For a multiphase sample, the  $^2\text{H}$  NMR spectrum is a superposition of the spectra of the individual phases, provided that the deuteron exchange between the phases is slow (as is

\* To whom correspondence should be addressed.

\* Abstract published in *Advance ACS Abstracts*, April 15, 1995.

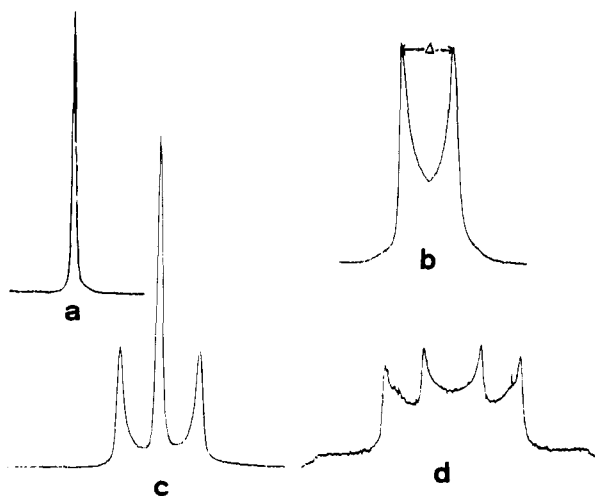


**Figure 1.** Some typical  $^2\text{H}$  NMR spectra for various samples of the copolymer  $\text{P}_{94}$ -water system at 298 K. Sample composition in weight percent polymer is given within brackets: (a)  $\nu_{1/2}$  (line width)  $\approx 10$  Hz,  $\text{L}_1$  phase (15%); (b)  $\Delta$  (splitting) = 63 Hz, E phase (55%); (c)  $\Delta = 55$  Hz, E + I two-phase region (40.5%); (d)  $\Delta_{\text{E}} = 75$  Hz and  $\Delta_{\text{D}} = 177$  Hz, D + E two-phase region.

usually the case). If the sample contains an anisotropic and an isotropic phase, the NMR spectrum consists of one splitting and a singlet (Figure 1c). In the same way, the sample containing a mixture of a lamellar and a hexagonal liquid crystal, two splittings will be generated in the  $^2\text{H}$  NMR spectrum (Figure 1d).  $^2\text{H}$  NMR has, therefore, become a standard technique for phase diagram determination.

$^2\text{H}$  NMR experiments were performed at constant temperature at a resonance frequency of 15.371 MHz (2.3 T) on a Bruker MSL 100 pulsed superconducting spectrometer working in the Fourier transform mode. The 10 mm i.d. NMR tube containing the sample ampule was placed in the NMR probe, and the sample was thermally equilibrated for at least 1 h before the spectrum was recorded. Thermal equilibration of the samples for 1 h was sufficient, since usually no variation in the NMR spectra was observed after 10 min at a given temperature. A  $\pi/2$  pulse (8  $\mu\text{s}$ ) with a pulse interval of 0.5 s and a dead time of 300  $\mu\text{s}$  was used. A total of 100–300 pulses was sufficient to obtain a quadrupole splitting. An observed quadrupole splitting ( $\Delta$ ) was measured in hertz as the peak-to-peak distance in a spectrum (see Figure 1b). The probe temperature was adjusted within  $\pm 0.5$  °C from 25 to 85 °C.

**Phase Diagram Determination.** The phase diagrams were determined by ocular inspection, by polarizing microscopy, and by analysis of  $^2\text{H}$  NMR spectra of deuterated water.

The samples were first examined by ocular inspection, against scattered light and between crossed polaroids for sample homogeneity and birefringency. In two-phase regions such as two liquid mixtures, one liquid and one cubic, or one liquid and one anisotropic liquid crystal, separation into the individual phases often occurs spontaneously, but this could also be augmented by centrifugation in an ordinary desk centrifuge.

The liquid crystalline phases were identified by examining the textures under the polarizing microscope (Axioplan Universal of Zeiss) equipped with a differential interference contrast (DIC) unit, a camera (MC 100) for direct imaging, and a video system with image analysis facilities for automatic documentation and registration of the results. For normal surfactant systems, a lamellar liquid crystal displays a mosaic planar texture, while a hexagonal liquid crystal shows a fanlike angular or a striated nongeometric texture.<sup>12</sup> No texture is displayed by a cubic liquid crystal, and only a black background is observed under a polarizing microscope. The texture of a liquid crystalline sample was first studied at room temperature, and the change in texture was then followed when the temperature was raised at a rate of about 2 °C/min.

The temperature was kept constant for several minutes at the transition between a single-phase and a two-phase region.

It is worthwhile mentioning that the textures displayed by the polymer liquid crystals in the present case are not as distinct as those displayed by normal surfactants. Two effects may be responsible for the weak textures: (i) the interior of the polymer aggregates is much less ordered than that of the surfactants; (ii) for the surfactant systems, the penetration of water in the aggregate interior is excluded, whereas for the copolymer aggregates, the penetration of water into the aggregates is implied.<sup>5</sup> This is easy to understand by noting that the hydrocarbon chains of the surfactants are much more hydrophobic in comparison with the PO blocks. Thus there are relatively smaller differences of polarity in the copolymers. The microdomain structure appears to be less well developed for the polymer liquid crystals. It is therefore necessary to temper the polymer sample for longer time in order to develop a distinct texture.

The identification of the hexagonal and lamellar liquid crystalline phases was also ascertained by comparing the magnitude of the  $^2\text{H}$  NMR splitting ( $\Delta$ ) of deuterated water. The observed quadrupolar splitting ( $\Delta$ ) for an anisotropic liquid crystalline sample is given by<sup>13</sup>

$$\Delta = \sum |P_i \nu_Q S_i| \quad (1)$$

where  $P_i$  is the fraction of  $^2\text{H}$  present at site  $i$  and  $(\nu_Q S_i)$  is the average quadrupole interaction at site  $i$ . It should be noted that  $(\nu_Q S_i)$  can be both positive and negative. For  $^2\text{H}$  in  $^2\text{H}_2\text{O}$ ,  $\nu_Q$  is independent of the site and is constant (220 kHz).<sup>14</sup> The observed variation in  $\Delta$  with sample composition therefore reflects changes in  $P_i$  and  $S_i$  which, however, can be difficult to separate. In the simplest model<sup>13,15</sup> only two sites are considered—water molecules bound ( $P_b$ ) to the EO groups and free water molecules ( $P_f$ ) tumbling without restriction. Hence, the order parameter for the free molecules vanishes, and eq 1 is simplified to

$$\Delta = |P_b \nu_Q S_b| \quad (2)$$

The order parameter  $S_b$  is given by the time average for the case of an axially symmetric electric field gradient<sup>13</sup>

$$S_b = \frac{1}{2} (3 \cos^2 \theta_{\text{MD}} - 1) \quad (3)$$

where  $\theta_{\text{MD}}$  is the time-dependent angle between the electric field gradient and the liquid crystal axis (the director). Relating the residual interaction to the local normal to the aggregate surface facilitates comparison between different phase structures. In the lamellar phase the director is perpendicular to the lamellae, and in the hexagonal phase it is parallel to the axes of the cylindrical aggregates. In the hexagonal phase, the rapid diffusion of deuterons around the cylindrical aggregates causes a further averaging of the expression in eq 3, and the absolute value of the order parameter is reduced by a factor of  $1/2$  due to this effect upon transition from a lamellar to a hexagonal liquid crystalline phase if all other factors are unaffected. Then, it follows from eq 2 as

$$\Delta_{\text{D}} = 2\Delta_{\text{E}} \quad (4)$$

(D and E refer to lamellar and hexagonal liquid crystalline phases, respectively) provided that (i)  $(P\nu_Q)_b$  is constant, (ii) the lamellae have no appreciable curvature, and (iii) the local interactions and molecular ordering are the same for the two phases.

For each phase diagram of the copolymer–water system, 15–20 samples were prepared, covering the whole concentration range for general observation at 25 °C. About 30 samples with different polymer concentrations were examined to determine the composition vs temperature phase diagram for each system. Within a single liquid crystalline phase region, NMR experiments were performed at a temperature interval

**Table 1. Polymorphism of EO-PO-EO Triblock Copolymers in Water at 298 K<sup>a</sup>**

polymer	$M_w$	formula	$f$	phases with increasing concns	CP (°C)
L <sub>62</sub>	2188	EO <sub>5</sub> PO <sub>30</sub> EO <sub>5</sub>	0.33	L <sub>1</sub> only	32
L <sub>31</sub>	1056	EO <sub>1</sub> PO <sub>17</sub> EO <sub>1</sub>	0.12	L <sub>1</sub> only	37
L <sub>61</sub>	1944	EO <sub>2</sub> PO <sub>30</sub> EO <sub>2</sub>	0.13	L <sub>1</sub> → L <sub>2</sub>	24
P <sub>85</sub>	4638	EO <sub>27</sub> PO <sub>39</sub> EO <sub>27</sub>	1.38	L <sub>1</sub> → I → E → D → L <sub>2</sub>	85
P <sub>94</sub>	4583	EO <sub>21</sub> PO <sub>47</sub> EO <sub>21</sub>	0.89	L <sub>1</sub> → I → E → D → L <sub>2</sub>	80
L <sub>64</sub>	2917	EO <sub>13</sub> PO <sub>30</sub> EO <sub>13</sub>	0.87	L <sub>1</sub> → E → V → D → L <sub>2</sub>	58
L <sub>92</sub>	3438	EO <sub>8</sub> PO <sub>47</sub> EO <sub>8</sub>	0.34	L <sub>1</sub> → E → D → L <sub>2</sub>	24

<sup>a</sup> Notes:  $f$  = (degree of polymerization of both EO blocks)/(degree of polymerization for the PO midblock); L<sub>1</sub>, L<sub>2</sub>, isotropic solution phases; E, hexagonal; D, lamellar, I and V, cubic liquid crystalline phases. CP refers to the cloud point and is given at 1 wt % polymer solution.

of 10 °C for each sample between 25 and 85 °C, and at phase transition, the temperature was adjusted carefully before the spectra were recorded. It was ensured that the samples attained thermal equilibrium at the temperature of observation.

## Results and Discussion

**General Phase Behavior.** Table 1 shows the general phase behavior of seven copolymer-water systems at 298 K. The existence of different phases is indicated as a function of the polymer concentration. L<sub>1</sub> represents an aqueous polymer solution, E is a hexagonal liquid crystalline phase, I and V are cubic liquid crystalline phases, D is a lamellar liquid crystalline phase, and L<sub>2</sub> is a concentrated polymer solution phase.

Below a  $M_w$  of about 2200, regardless of composition  $f$ , no liquid crystalline phases, but only solution phases, are observed (see the first three copolymers in Table 1). By heating these systems up to the cloud points, no liquid crystalline phases have been detected (similar to the simple nonionic surfactants, the aqueous solubility of EO-containing polymers, such as PEO and Pluronics, decreases with increasing temperature, displaying a clouding temperature, termed as the cloud point). This observation is expected since it is a general feature for the block copolymer systems. The formation of liquid crystalline phases requires a minimum  $M_w$  in order to satisfy the requirement of a minimum hydrophobic part as well as a balance between the hydrophobic and hydrophilic forces.<sup>16</sup>

It is well-known that the aggregate formation stems from the segregative effect which depends on block-block interaction, described by  $N\chi_{AB}$ , and copolymer-solvent interaction, described by  $N_A\chi_{A1} + N_B\chi_{B1}$  ( $\chi$  is the Flory interaction parameter per polymer segment and 1 refers to the solvent). Therefore, for a given system, the segregative effect decreases with decreasing  $M_w$  of the copolymer. When  $M_w$  of the copolymer is sufficiently low, no micelles or only smaller micelles would be formed. On the other hand, as micelles become sufficiently small, the gain in mixing entropy by forming a homogeneous phase becomes high and dominant, which destabilizes the mesophases. This argument is supported by investigations on the micellization of different Pluronic copolymers in water. It has been shown, both theoretically<sup>17</sup> and experimentally,<sup>18</sup> that a decrease in  $M_w$  of copolymers, regardless of the composition  $f$ , leads to less negative free energies of micellization, indicating a weaker propensity to form micelles with decreasing  $M_w$ .

As  $M_w$  becomes sufficiently high, several liquid crystalline phases appear (see last four polymer systems in

Table 1). The phase behavior can be divided broadly into three types. Type I is displayed by the P<sub>94</sub>-water and P<sub>85</sub>-water systems. Both P<sub>94</sub> and P<sub>85</sub> possess relatively high values of  $f$  and  $M_w$  and high cloud points (above 80 °C). The sequence of phases with increasing copolymer concentration at 298 K is aqueous polymer solution (L<sub>1</sub>) → cubic liquid crystalline phase (I) → hexagonal liquid crystalline phase (E) → lamellar liquid crystalline phase (D) → concentrated polymer solution phase (L<sub>2</sub>). Type II is displayed by the L<sub>64</sub>-water system. L<sub>64</sub> possesses a high value of  $f$  but relatively low  $M_w$  (EO and PO blocks are therefore shorter than those of P<sub>94</sub> and P<sub>85</sub>). Its cloud point is at about 58 °C. There are two main differences between types I and II: (i) the first ordered phase appearing in type I is the cubic phase (I), while in type II the hexagonal phase (E) first appears; (ii) in type I the cubic phase (I) appears between the L<sub>1</sub> and E phases, while in type II the cubic phase (V) appears between the E and D phases. The cubic phase I is stiff, while the V phase is relatively soft. The microstructures of the cubic phases, I and V, are expected to be different<sup>16,19,20</sup> (see later). Type III is displayed by the L<sub>92</sub>-water system. L<sub>92</sub> possesses a low value of  $f$  and a low cloud point (CP ≈ 24 °C). The main features of types II and III are the same except that no cubic phase is detected for type III.

In addition to the molecular weight ( $M_w$ ), the copolymer composition, represented by  $f$  = (degree of polymerization for both EO blocks)/(degree of polymerization for the PO midblock), also plays an important role in determining the phase behavior. Changes in  $f$  primarily affect the shape and packing symmetry of the ordered microstructure by changing the chain stretching constraints on each side of the interface. The presence of a solvent should simply result in an increase in the apparent volume of the soluble blocks and, therefore, an enhancement in the repulsion among the soluble groups (EO groups in the present systems). When the apparent volume of soluble blocks is much larger than that of insoluble blocks (PO blocks in the present systems), spherical or cylinder micelles, and the I or the E phases, are favored. Such behavior is easy to understand by noting that the space offered on the convex side of the interface is larger than the corresponding space on the concave side. When the relative length of insoluble blocks is sufficiently large ( $f$  is small), bilayer, even reversed, structure is favored.

With an establishment of a general picture of the phase behavior, we now examine the phase behavior of two systems, L<sub>64</sub>-water and P<sub>94</sub>-water, in more detail.

**EO<sub>21</sub>PO<sub>47</sub>EO<sub>21</sub> (P<sub>94</sub>)-Water System.** The binary phase diagram of the EO<sub>21</sub>PO<sub>47</sub>EO<sub>21</sub> (P<sub>94</sub>)-water system is shown in Figure 2. Below the cloud point (80 °C), the system forms an isotropic solution phase (L<sub>1</sub>) which coexists with a viscous cubic liquid crystalline phase (I) at about 22 wt % of the polymer. The I phase is stable between 24 and 39 wt % of the polymer. Between 39 and 41 wt % of polymer, there appears a narrow two-phase region, I + E, which is followed by a hexagonal liquid crystalline phase (E) (41–60 wt % of the polymer). The system also yields a lamellar liquid crystalline phase (D) between 70 and 85 wt % of the polymer. Phase D is in equilibrium with phase E on the water-rich part and with a polymer concentrated solution phase (L<sub>2</sub>) on the water-poor part.

On increasing the temperature, both the I and E phases swell with water. However, the thermal stability of the I phase is low, and above ca. 45 °C, phase I

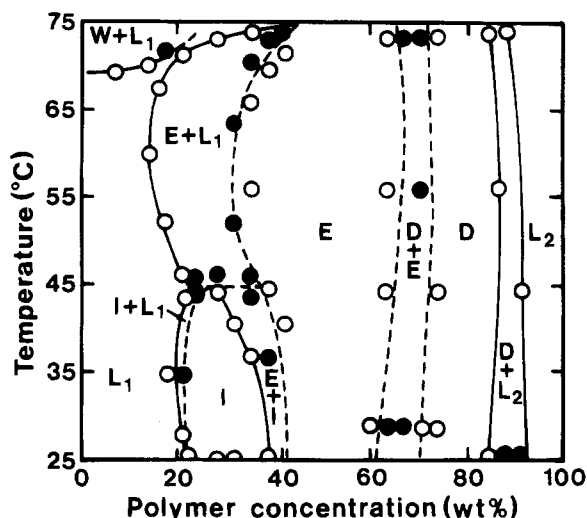


**Figure 2.** Binary phase diagram (composition vs temperature) for the system  $P_{94}$  ( $EO_{21}PO_{47}EO_{21}$ )-water. Notations are as follows:  $L_1$ ,  $L_2$ , W, isotropic solution phases; E, hexagonal; D, lamellar; I, cubic liquid crystalline phases; D + E, E + I, etc., two-phase regions. Solid border lines are accurate to  $\pm 1\%$ , and broken border lines are less accurate.

melts and forms either a two-phase region,  $L_1 + E$ , or an E phase via the  $L_1 + E$  two-phase region, depending on sample compositions. No swelling of phase D with water is, however, observed on heating. The viscosity of the solution phase,  $L_1$ , is found to increase with increasing temperature, and near the two-phase region,  $L_1 + E$ , at higher temperature, the isotropic samples on rotating suddenly display a birefringency between the crossed polaroids. Both the E and D phases melt at about 78 and 85 °C, respectively, giving rise to a narrow isotropic solution one-phase region (this has not been indicated in the phase diagram), which is followed by a liquid-liquid two-phase region at higher temperature.

**$EO_{13}PO_{30}EO_{13}$  ( $L_{64}$ )-Water System.**  $L_{64}$  and  $P_{94}$  have identical compositions ( $f \approx 0.9$ ). But the chain length of the former is shorter than that of the latter. The main features of the binary phase diagram for these two systems are similar (Figure 3). There are two two-phase regions,  $L_1 + E$  and  $L_2 + D$ , between single phases  $L_1$  and E and between  $L_2$  and D, respectively. These two-phase regions are very narrow and included within the respective liquid crystalline phase. The two-phase region D + E is also extremely narrow. We have succeeded in obtaining two splittings on the  $^2H$  NMR spectrum at one polymer concentration only over the entire temperature range, and the border line is drawn between phase E and phase D at this concentration. Like  $P_{94}$ ,  $L_{64}$  forms two isotropic solution phases,  $L_1$  and  $L_2$ , two anisotropic liquid crystalline phases, E and D, and one cubic liquid crystalline phase, V. However, there are two main differences distinguishing the  $L_{64}$ -water system from the  $P_{94}$ -water: (i) the first ordered phase to appear with increasing the polymer concentration at room temperature is the E phase for the  $L_{64}$ -water system, while phase I is the first one for the system  $P_{94}$ -water; (ii) for the  $L_{64}$ -water system, the cubic phase (V), which has a very limited range of existence, appears between the E and D phases. In fact the stability range is so narrow that it is difficult to prepare samples containing a single cubic liquid crystal. Most of the samples prepared are mixtures of either V + E or V + D. Moreover, the thermal stability of the V phase for this system is low (below 25 °C) compared to

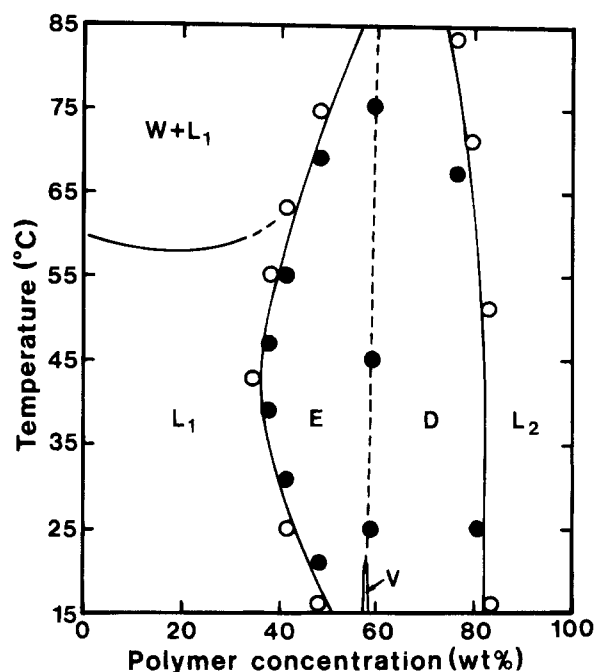


**Figure 3.** Binary phase diagram (composition vs temperature) for the system  $L_{64}$  ( $EO_{13}PO_{30}EO_{13}$ )-water. Notations are as in Figure 2, and the V is cubic liquid crystalline phase. Narrow two-phase regions are included with liquid crystalline regions.

that of the I phase (45 °C) characterized for the  $P_{94}$ -water system. For the latter case, the cubic phase is also stable over a wider concentration range.

Cubic phases occur frequently in surfactant and surfactant-like lipid systems,<sup>19,20</sup> and in different block copolymer systems.<sup>21-23</sup> Mainly, two different types, each appearing in different regions of the phase diagram, have been studied extensively. Their structures are related in some manner to those of adjacent phases. It is established that the cubic phase that appears between the micellar solution and the hexagonal phase (like the I phase in the  $P_{94}$ -water system; Figure 2) consists of small micelles, probably of spherical shape, packed in body-centered (bcc) or face-centered cubic (fcc) arrays; the other type of cubic phase, which consists of a bicontinuous network with water and surfactant (or block copolymer) forming bicontinuous zones, can be found between the hexagonal and lamellar phases (like the V phase in the  $L_{64}$ -water system; Figure 3). Although the microstructure of either the I or V phase in this paper has not been studied, we believe, from the arguments just mentioned above, that the I phase possesses a bcc (or fcc) structure while the V phase possesses a bicontinuous type structure. At this point, it is worthwhile noting that the existence of the bicontinuous type cubic phase has been demonstrated only recently, in starblock copolymers,<sup>24</sup> diblock copolymers,<sup>22</sup> and diblock<sup>25</sup> or triblock<sup>26</sup> copolymer/homopolymer blends over a relatively narrow concentration range. To our knowledge, this is the first report that a cubic phase that may have a bicontinuous structure has been identified between the hexagonal and lamellar phases in triblock copolymer-solvent systems. As mentioned earlier, the distinction between the hydrophobic and hydrophilic parts of a Pluronic copolymer molecule is not as clear-cut as in a surfactant molecule. This may result in the fact that the microstructures of cubic phases in the copolymer systems may be different from those in the surfactant systems.

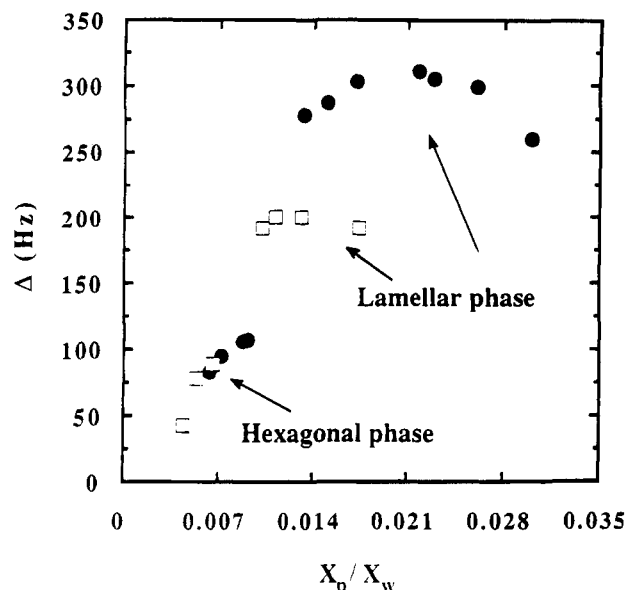


**Figure 4.**  $^2\text{H}$  NMR splitting ( $\Delta$ ) of deuterated water vs molar ratio between polymer and water,  $X_p/X_w$ , for the systems  $L_{64}$ -water (filled circles) and  $P_{94}$ -water (open squares). The experimental temperature was 298 K.

**$^2\text{H}$  NMR in Liquid Crystal.** The observed quadrupole splittings in liquid crystalline phases can be further analyzed by the conventional two-site model within a division into "free" and "bound" water molecules. Assuming that there is a fast exchange between the free and bound water within the NMR time scale and the ordering of free water molecules is negligible, we may express the splitting ( $\Delta$ ) in eq 2 as a function of the molar ratio between polymer,  $X_p$ , and water,  $X_w$ , as<sup>15,27</sup>

$$\Delta = n |(\varphi_Q S_b)| \frac{X_p}{X_w} \quad (5)$$

where  $n$  is the hydration number and the other terms are as defined previously.

Some representative  $\Delta$  values for the  $L_{64}$ -water and  $P_{94}$ -water systems at 25 °C are presented in Figure 4 as a function of the molar ratio between polymer,  $X_p$ , and water,  $X_w$ . In the hexagonal phase (E) region (where  $X_p/X_w$  is below ca. 0.008 for the  $P_{94}$ -water system and ca. 0.01 for the  $L_{64}$ -water system) there is an increase of the  $\Delta$  values with increasing  $X_p/X_w$ , and, furthermore, extrapolation of the  $\Delta$  values passes approximately through the origin, as predicted by eq 5.  $\Delta$  values observed in the lamellar (D) phase (where  $X_p/X_w$  is above ca. 0.009 for the  $P_{94}$ -water system and ca. 0.013 for the  $L_{64}$ -water system) are much larger than those in the E phase region. We have also recorded double splittings within a narrow concentration region, showing the coexistence of the E and D phases; the larger splitting corresponds to the D phase, and the smaller one, to the E phase.

From eq 5 a value of the order parameter,  $S_b \approx 10^{-2}$  is calculated by using the splitting value measured in the hexagonal phase region and  $n = 6$ . The value obtained for the present systems is a little higher than the value reported in the E phase for the surfactant systems.<sup>28</sup> It appears that water is more ordered in the present systems.

Further analysis of the splitting values show deviations from the two-site model. For example, no linear

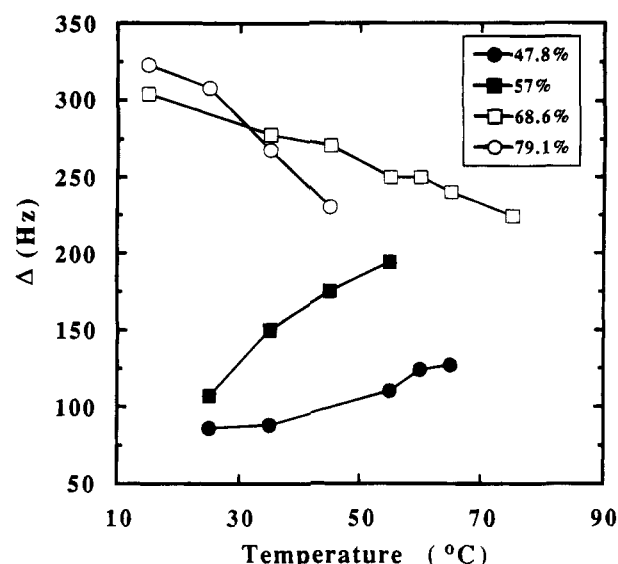


**Figure 5.**  $^2\text{H}$  NMR splitting ( $\Delta$ ) of deuterated water vs temperature for the system  $L_{64}$ -water. Filled circles and squares refer to the hexagonal phase and open circles and squares to the lamellar phase.

increase of the splitting values with increased polymer concentration is obtained in the lamellar phase region.

Deviations from the two-site model have also been reported for liquid crystals formed in the water-poor part of the surfactant systems.<sup>29</sup> This is explained on the basis that most of the water is associated with the polar head groups of the surfactant aggregates, thus invalidating the assumption of fast exchange between the free and bound water molecules as well as of the constant hydration number. A similar argument can be put forward for the present system. For example, assuming a hydration number of 6 per EO group,<sup>30</sup> it can be shown that all the water would be associated with the EO groups at the polymer concentrations above 50 wt %.

We have also measured the splitting values in the D and E phases at different temperatures. Figure 5 shows the  $\Delta$  values of a few representative samples in the hexagonal and lamellar phases of the  $L_{64}$ -water system between 15 and 70 °C. A reduction of splitting values with increasing temperature is recorded for the D phase, while a reverse trend is observed for the E phase. The reduction of the  $\Delta$  values may be understood in terms of dehydration of the EO groups as the temperature is increased. This finding is in agreement with previous results reported for the Pluronic aggregates in isotropic solutions.<sup>6,31</sup> Malmsten and Lindman<sup>31</sup> have measured an increase of the water diffusion coefficient for the polymer solution of  $\text{EO}_{99}\text{PO}_{65}\text{EO}_{99}$  with increased temperature. The diffusion data are found to be in good agreement with a gradual dehydration of the polymer molecules with increasing temperature. However, it is not straightforward to understand the increase of splitting values with increased temperatures. It is to be noted that the hexagonal phase is formed at high water contents and the polar EO groups are hydrated more extensively compared to those in the lamellar phase. The interaction between completely hydrated EO groups is shown to be repulsive at low temperature.<sup>32,33</sup> When the temperature is increased, the interaction between the polar groups becomes less repulsive. This is probably accompanied by a gradual change of the conformation of the polar parts of the polymer as the distance between the head groups is decreased and the EO

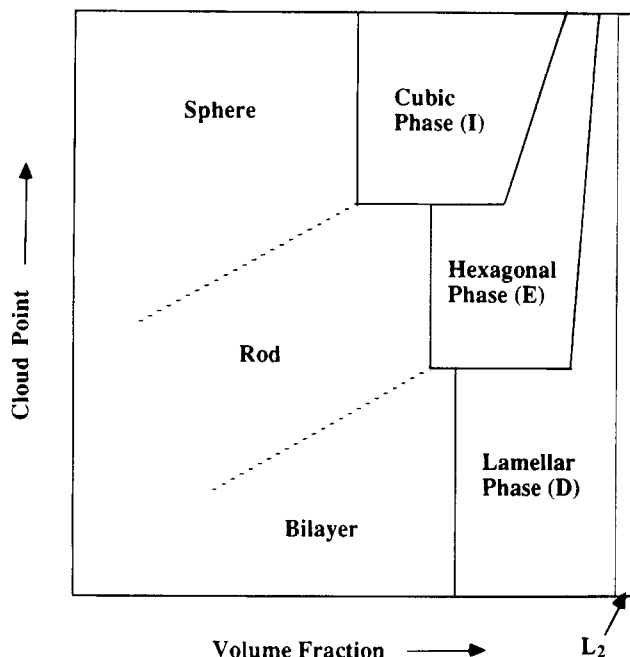


**Figure 6.** Schematic illustration of mesophase structures vs volume fraction and cloud point of the polymer.

chains become more extended, pointing out from the aggregate surface. This will, of course, change the quantity  $n[(\partial Q S)_b]$ . The number of bound water molecules might, as mentioned above, decrease, but if  $[(\partial Q S)_b]$  increases more, this can explain the increased  $\Delta$  values measured in the E phase with increased temperature. Increased  $\Delta$  values with increased temperatures reported for the surfactant–water system are also explained in terms of changing the order parameter ( $S_b$ ) with temperature.<sup>34</sup>

### Concluding Remarks

It has been demonstrated that formation of liquid crystalline phases above certain polymer concentrations is a rather common feature for the Pluronic copolymer–water systems. Four factors are important for controlling the phase behavior. They are molecular weight, composition, temperature, and concentration.

It may be recalled that Pluronic polymers have a reverse solubility in water with increasing temperature, and the cloud points of polymers depend also on the structural parameters,  $M_w$  and  $f$ . It should not be unexpected that the microstructures of the aggregates and mesophases are related to the cloud point of the polymer. At a given  $M_w$ , increasing  $f$  always corresponds to an increase in the cloud point.<sup>35</sup> Above the  $M_w$  threshold for the establishment of the mesophase it is reasonable to say that (i) for the polymers having sufficiently high cloud point, spherical aggregates are dominant and only the cubic phase (I) with a relatively wide concentration and temperature stability range is expected, (ii) while for polymers having sufficiently low cloud point, bilayer aggregates and the lamellar (D) phase are dominant, and (iii) for polymers having intermediate cloud point, the aggregate structure can be easily changed as the polymer concentration is varied, showing rich varieties in the phase behavior. The polymers used in the present paper belong to this type

(see the last four polymers in Table 1). The relationship between cloud point of the polymer and mesophase structures is illustrated schematically in Figure 6. At this point, it is worthwhile noting that the arguments above hold for nonionic surfactant–water systems as well.<sup>36</sup>

**Acknowledgment.** S. Johansson is acknowledged for his technical assistance. Prof. B. Lindman and Dr. P. Linse are thanked for valuable comments on the manuscript. This work is financed by The Swedish Research Council for Engineering Science (TFR).

### References and Notes

- (1) Al-saden, A. A.; Whateley, T. L.; Florence, A. T. *J. Colloid Interface Sci.* **1982**, *90*, 303.
- (2) Mortensen, K.; Brown, W. *Macromolecules* **1993**, *26*, 4128.
- (3) Zhou, Z.; Chu, B. *J. Colloid Interface Sci.* **1988**, *126*, 171.
- (4) Zhou, Z.; Chu, B. *Macromolecules* **1988**, *21*, 2548.
- (5) Almgren, M.; Alsins, J.; Bahadur, P. *Langmuir* **1991**, *7*, 446.
- (6) Linse, P. *J. Phys. Chem.* **1993**, *97*, 13896.
- (7) Malmsten, M.; Lidman, B. *Macromolecules* **1993**, *26*, 1282.
- (8) Mortensen, K.; Brown, W.; Norden, B. *Phys. Rev. Lett.* **1992**, *68*, 2340.
- (9) Mortensen, K. *Europhys. Lett.* **1992**, *19*, 599.
- (10) Persson, N.-O.; Fontell, K.; Lindman, B.; Tiddy, G. J. T. *J. Colloid Interface Sci.* **1975**, *53*, 461.
- (11) Ulmius, J.; Wennerström, H.; Lindblom, G.; Arvidson, G. *Biochemistry* **1977**, *16*, 5742.
- (12) Rosevear, F. B. *J. Am. Oil chem. Soc.* **1954**, *31*, 628.
- (13) Wennerström, H.; Lindman, B.; Lindholm, G. *Chem. Scr.* **1974**, *6*, 97.
- (14) Glasel, J. A. In *Water, a Comprehensive Treatise*; Franks, F., Ed.; Plenum Press: New York, 1972; Vol. I, p 215.
- (15) Wennerström, H.; Persson, N.-O.; Lindman, B. In *Colloidal Dispersions and Micellar Behavior*; Mittal, K. L., Ed.; ACS Symposium Series 9; American Chemical Society: Washington, DC, 1975; p 253.
- (16) Leibler, L. *Macromolecules* **1980**, *13*, 1602.
- (17) Linse, P. *Macromolecules* **1993**, *26*, 4437.
- (18) Alexandridis, P.; Holzwarth, J. F.; Hatton, T. A. *Macromolecules* **1994**, *27*, 2414.
- (19) Luzzati, V.; Spegt, P. A. *Nature* **1967**, *215*, 701.
- (20) Fontell, K. *Adv. Colloid Interface Sci.* **1992**, *41*, 127.
- (21) Bates, F. S. *Science* **1991**, *251*, 898.
- (22) Hasegawa, H.; Tanaka, H.; Yamasaki, K.; Hashimoto, T. *Macromolecules* **1987**, *20*, 1641.
- (23) Herman, D. S.; Kinning, D. J.; Thomas, E. L.; Fetter, L. J. *Macromolecules* **1987**, *20*, 2940.
- (24) Thomas, E. L.; Alward, D. B.; Kinning, D. J.; Martin, D. C.; Handlin, D. L.; Fetters, L. J. *Macromolecules* **1986**, *19*, 2197.
- (25) Winey, K. I.; Thomas, E. L.; Fetters, L. J. *Macromolecules* **1992**, *25*, 422.
- (26) Xie, R.; Yang, B. X.; Jiang, B. Z. *Macromolecules* **1993**, *26*, 7099.
- (27) Khan, A.; Fontell, K.; Lindblom, G.; Lindman, B. *J. Phys. Chem.* **1982**, *86*, 4266.
- (28) Khan, A.; Fontell, K.; Lindblom, G. *J. Phys. Chem.* **1982**, *86*, 383.
- (29) Khan, A.; Fontell, K.; Lindman, B. *J. Colloid Interface Sci.* **1984**, *101*, 193.
- (30) Sadaghiani, A. S.; Khan, A. *Langmuir* **1991**, *7*, 898.
- (31) Malmsten, M.; Lindman, B. *Macromolecules* **1992**, *25*, 5446.
- (32) Kjellander, R.; Florin, E. *J. Chem. Soc., Faraday Trans. 1* **1981**, *77*, 2053.
- (33) Kjellander, R. *J. Chem. Soc., Faraday Trans. 2* **1982**, *78*, 2025.
- (34) Ikeda, K.; Khan, A.; Meguro, K.; Lindman, B. *J. Colloid Interface Sci.* **1989**, *133*, 192.
- (35) Pluronic & Tetronic Block Copolymer Surfactants (BASF), 1989, Product Information Publication.
- (36) Mitchell, D. J.; Tiddy, G. J. T.; Waring, L.; Bostock, T.; McDonald, P. M. *J. Chem. Soc., Faraday Trans. 1* **1983**, *79*, 975.

MA946173O